Available online at www.sciencedirect.com
SCIENCE DIRECT®
ELSEVIER
Pattern Recognition Letters 26 (2005) 2424–2430
Pattern Recognition Letters
www.elsevier.com/locate/patrec

# Fingerprint matching combining the global orientation field with minutia

Jin Qi [a,b,*], Suzhen Yang [c], Yangsheng Wang [b]

[a] Department of Electrical Engineering, University of Electronic Science and Technology of China, Chengdu 610054, PR China
[b] National Laboratory of Pattern Recognition, Institute of Automation, Chinese Academy of Sciences, Beijing 100080, PR China
[c] Department of Foreign Language, Chengdu Institute of Technology, Chengdu 610050, PR China

Received 21 May 2004; received in revised form 26 March 2005
Available online 17 June 2005

Communicated by H. Wechsler

**Abstract**

We define a novel feature vector for each fingerprint minutia based on the global orientation field. These features are used to identify corresponding minutiae between two fingerprint impressions by computing the Euclidean distance between vectors. A novel fingerprint matching algorithm is developed using both the orientation field and minutia. A series of experiments conducted on the public data collection, DB3, FVC2002, demonstrates the effectiveness of our method.


*Keywords:* Fingerprints; Matching; Features; Orientation field

## 1. Introduction

Fingerprint matching techniques can be broadly classified as being minutiae-based or correlation-based. In general, it has been observed that minutiae-based methods perform better than correlation-based ones. So most fingerprint verification systems required to provide a high processing speed and high degree of security are so far based on minutia matching.

But minutiae-based matching is essentially the famous point pattern match problem that is generally intractable because it encounters the minutiae correspondence problem. The minutiae correspondences can be quite difficult to obtain due to

* Corresponding author. Address: National Laboratory of Pattern Recognition, Institute of Automation, Chinese Academy of Sciences, Beijing 100080, PR China. Fax: +8610 82619272.

*E-mail addresses:* jqi@nlpr.ia.ac.cn (J. Qi), wys@nlpr.ia.ac.cn (Y. Wang).

0167-8655/$ - see front matter © 2005 Elsevier B.V. All rights reserved.
doi:10.1016/j.patrec.2005.04.016

several factors such as the rotation, translation and deformation of the fingerprints, the location and direction errors of the detected minutiae as well as the presence of spurious minutiae and the absence of genuine minutiae.

Several minutiae matching approaches have been proposed in the literature. These include methods based on structure matching (Chen and Kuo, 1991; Hrechak and McHugh, 1990; Jiang and Yau, 2000; Wahab et al., 1998), alignment matching (Jain et al., 1997a,b; Ratha et al., 1996; Ross et al., 2003), non-linear transformation (Almansa and Cohen, 2000; Bazen and Gerea, 2002). The key aspect of all these methods is to obtain the minutiae correspondences accurately. The methods proposed in (Jain et al., 1997a,b; Ratha et al., 1996; Ross et al., 2003) make use of ridges associated with each minutia to get the correspondences. However, the ridge is less discriminatory feature because the ridges from different fingers or different positions in the same fingerprint may be very similar. The local structure composed of several minutiae close to each other serves to obtain the minutiae correspondences in (Chen and Kuo, 1991; Hrechak and McHugh, 1990; Jiang and Yau, 2000; Wahab et al., 1998; Almansa and Cohen, 2000; Bazen and Gerea, 2002). It is noted that the representation of local structure based on a group of minutiae is not robust because it relies on the interdependencies between minutia details, which can be missed or erroneously detected by a minutia extraction algorithm. In addition, determining the similarity of local structures is difficult because the correspondences between the elements in local structures cannot be known.

With these in mind, we develop a new method of fingerprint matching incorporating the global orientation field with minutiae properly. In contrast to the local structural features employed by the matching algorithms proposed in (Chen and Kuo, 1991; Hrechak and McHugh, 1990; Jiang and Yau, 2000; Wahab et al., 1998), the novel structure of each minutia we construct in this paper is not sensitive to noise because it only depends on the global fingerprint orientation field which is relatively robust to noise. Furthermore, our structure capturing the rich information on fingerprint ridge-flow pattern is more discriminative than the local minutia structure. It is exciting that our structure can be represented as a fixed-size minutia feature vector. Hence, obtaining the correct minutiae correspondences exactly becomes the computation of Euclidean distances between feature vectors. The task is straightforward.

It is well known that many existing minutia-based fingerprint matching techniques only use minutiae to measure the similarity of two fingerprints. In this paper, a novel fingerprint matching algorithm is developed using both the orientation field and minutia. The final matching score measures both the number of matching minutia pairs and similarity degree of two orientation fields. It helps to decrease both the false acceptance rate (FAR) and the false reject rate (FRR) simultaneously because our method takes advantage of more information than traditional minutiae based matching methods.

The rest of the paper is organized as follows. A detailed definition of our novel minutiae feature vector is presented in the following section. The matching scheme based on the proposed minutia structure is developed in Section 3. This is followed by validation experiments conducted on the public domain collection of fingerprint images, DB3, FVC2002. Finally, concluding remarks are presented in Section 5.

## 2. Definition of the novel structure

In general, a minutia point $M$ detected from a fingerprint can be described by a feature vector given by:

$$F = (x \quad y \quad \omega), \tag{1}$$

where $(x, y)$ is its coordinate, $\omega$ is the local ridge direction.

Generally, the orientation of fingerprint ridge is in the range $[-\pi/2, \pi/2]$ or $[0, \pi]$. Here it is assumed that the value of ridge orientation is from $-\pi/2$ to $\pi/2$. For measuring the difference of two ridge directions $\omega_1$ and $\omega_2$, we define a function $d(\omega_1, \omega_2)$ as the value of $\omega_2$ subtracted from $\omega_1$. Considering that the difference of 30° may result in the difference of $-150°$ due to the effect of rotation of fingerprint image on the directions of ridges. Hence, the function $d(\omega_1, \omega_2)$ can be given as follows:

$$d(\omega_1,\omega_2) = \begin{cases} \omega_1-\omega_2 \\ \quad \text{if } -\pi/2<(\omega_1-\omega_2)<\pi/2, \\ \omega_1-\omega_2+\pi \\ \quad \text{if } -\pi<(\omega_1-\omega_2)<-\pi/2, \\ \omega_1-\omega_2-\pi \\ \quad \text{if } \pi/2<(\omega_1-\omega_2)<\pi. \end{cases} \tag{2}$$

Given a minutia point $M$ with orientation $\omega$, we define our minutia structure as following procedures.

Let $\theta_1 = \omega$, $\theta_2 = \theta_1 + 2\pi/3$ and $\theta_3 = \theta_2 + 2\pi/3$. We plot three lines $l_1$, $l_2$, and $l_3$ along the angles $\theta_1$, $\theta_2$ and $\theta_3$ with respect to $X$ axis through the minutia point $M$. A sampling step is done starting with the minutia point $M$ along each line with sampling interval $\tau$. The sampling action along each line stops till the latest sampling point falls in fingerprint background region, as illustrated in Fig. 1.

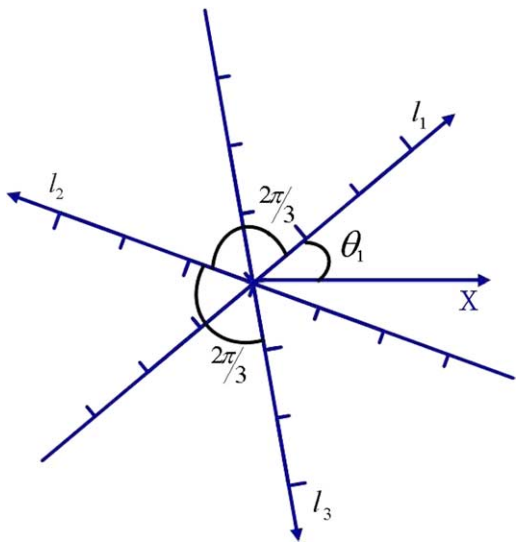


Fig. 1. Sampling points organized on three lines around a minutia detail: the central intersection point is fingerprint minutia; the $X$ axis is horizontal axis; $\theta$ is the orientation of minutia; the crossing angle among the three lines $l_1$, $l_2$, $l_3$ is $\pi/3$; the short line segments on each straight line indicate the sampling points.

The sampling pattern consists of three lines $l_m$, $(1 \leqslant m \leqslant 3)$ with three positive directions $\theta_m$, $(1 \leqslant m \leqslant 3)$, each one of them comprising $N_m$ sampling points $P_m^k$, $(1 \leqslant k \leqslant N_m,\ 1 \leqslant m \leqslant 3)$, equally distributed along the line $l_m$. Denoting by $\omega_m^k$ the local ridge orientation estimated in $P_m^k$, the relative direction $\psi_m^k$ between minutia $M$ and the sampling point $P_m^k$ calculated by

$$\psi_m^k = d(\omega, \omega_m^k) \tag{3}$$

is independent from the rotation and translation of the fingerprint. The feature vector $F$ of a minutia $M$ that describes its structure characteristic with global fingerprint orientation field is given by

$$F = \{\{\psi_m^k\}_{i=1}^{N_m}\}_{m=1}^{3}. \tag{4}$$

The structure feature vector $F$ is invariant to rotation and translation of the fingerprint. Note that the number of sampling points on each line for different minutiae may be different. But the sampling points on each line can be ordered according to the distance from the central minutia to the sampling points. Therefore, it is easy to find the corresponding components between two feature vectors using the minutia orientation and the distance from sampling point to central minutia as a reference.

Suppose $F_i$ and $F_j$ are the structure feature vectors of minutia $i$ from input fingerprint and minutia $j$ from template fingerprint, respectively. A similarity level is defined as

$$S(i,j) = \begin{cases} \dfrac{T-|F_i-F_j|}{T}, & \text{if } |F_i-F_j|<T, \\ 0, & \text{otherwise}, \end{cases} \tag{5}$$

where $T$ is the predefined threshold and $|F_i - F_j|$ is the Euclidean distance between these two feature vectors. Note that the dimensions of the two feature vectors may be different. So the Euclidean distance is computed only using the corresponding components between them. If there is no corresponding counterpart of some element of one feature vector, the element will be discarded when computing the Euclidean distance involving the feature vector. The similarity level $S(i,j)$, $0 \leqslant S(i,j) \leqslant 1$, describes a matching certainty level of a structure pair instead of simply matched or not matched. $S(i,j) = 1$ implies a perfect match while $S(i,j) = 0$ implies a total mismatch.

## 3. Fingerprint matching

Using the proposed minutia feature vectors, we develop a new fingerprint matching algorithm making use of both fingerprint minutiae and orientation fields. Different from other minutia-based approaches our algorithm receives at the input two minutia lists and two orientation fields captured from two fingerprint impressions and delivers a matching score that expresses the degree of similarity between the two fingerprints. In order to align two point sets and two orientation fields before calculating the matching score, we need to identify a set of corresponding minutia pairs.

### 3.1. Corresponding minutia identification

The value of the similarity level between minutiae serves to identify corresponding pairs. The best-matched structure pair can be used as a corresponding point pair. Although not all well-matched structures are reliable, our experiments show that the best-matched structure pair of all minutia structures of template and input fingerprints is very reliable. The best-matched minutia structure pair $(b_1, b_2)$ is obtained by maximizing the similarity level as

$$S(b_1, b_2) = \max_{i,j}(S(i,j)). \tag{6}$$

### 3.2. Registration

The registration stage is meant to recover the geometric transformation between the two fingerprint impressions.

In our work, the rigid transformation, i.e., translation vector ($t = [t_x, t_y]^{\mathrm{T}}$) and rotation angle ($\psi$), is recovered by the best-matched structure pair that exhibits the largest similarity value in Eq. (6). Let the best-matched minutia structure pair is denoted by $(b_1, b_2)$, minutia $b_1$ from the input fingerprint and another $b_2$ from the template fingerprint. Hence we have

$$\psi = D(b_2) - D(b_1), \quad \text{and} \quad t = P(b_2) - R_\psi P(b_1), \tag{7}$$

where $R_\psi$ denotes the $2 \times 2$ operator of counterclockwise rotation with $\psi$ and the position and direction of a minutia $b$ are denoted by $P(b) = [x(b), y(b)]^{\mathrm{T}}$ and $D(b)$, respectively. Applying the estimated geometric transformation onto the minutiae from the test fingerprint we obtain the list comprising the registered minutiae. Also, The orientation field from the test fingerprint will be aligned using the estimated transformation simultaneously.

### 3.3. Minutia pairing

Because of various factors that include the presence of local non-linear deformations and the errors induced by the minutia extraction algorithm, the corresponding minutiae cannot overlap exactly. Consequently, one must allow a certain tolerance between the positions and directions of corresponding minutiae by employing an elastic matching algorithm as proposed in (Jiang and Yau, 2000; Jain et al., 1997b; Ratha et al., 1996). Therefore, the matching should be elastic by using a 3-D bounding box $B_g$ in the feature space instead of an exact matching. In our method, the corresponding minutiae pairs are collected among the pairs with the largest similarity level values in Eq. (5), which, also fall in the bounding box $B_g$.

### 3.4. Orientation block pairing

As the orientation field estimation algorithm proposed in (Jain et al., 1997b), the fingerprint image should be divided into a number of sub-blocks and compute the orientation of each sub-block. fingerprint orientation field is composed of these sub-blocks. With the registered orientation field, the procedure to identify the corresponding orientation block pairs is straightforward. Let $(B_1, B_2)$ denote the corresponding orientation block pair, block $B_1$ from test fingerprint, block $B_2$ from template fingerprint, respectively. The similarity degree $S(B_1, B_2)$ of the two blocks $B_1$ and $B_2$ is calculated as follows:

$$\phi(B_1, B_2) = |O(B_1) + \psi - O(B_2)|, \tag{8}$$

$$S(B_1, B_2) = \begin{cases} \dfrac{T_1 - \phi(B_1, B_2)}{T_1}, & \text{if } \phi(B_1, B_2) < T_1, \\ 0, & \text{others}, \end{cases} \tag{9}$$

where $\psi$ is computed with Eq. (7), $T_1$ is a threshold and the direction of a block $B$ is denoted by $O(B)$.

### 3.5. Matching score computation

With the introduction of our novel minutia structures and registered fingerprint orientation fields the matching score $M_s$ can be determined by both minutia matching score $M_m$ and orientation field matching score $M_o$.

Let $N_1$ and $N_2$ denote the number of minutiae located inside the intersection of the two fingerprint images for test and template fingerprints, respectively. The minutia matching score $M_m$ can be calculated according to the following equation:

$$M_m = \frac{\sum_{i,j} S(i,j)}{\max\{N_1, N_2\}}, \tag{10}$$

where $(i,j)$ is the corresponding minutiae pair, one from test fingerprint and another from template fingerprint, respectively, and $S(i,j)$ is computed according to Eq. (5).

The orientation field matching score $M_o$ is defined by

$$M_o = \frac{\sum_{B_i,B_j} S(B_i, B_j)}{N}, \tag{11}$$

where $(B_i, B_j)$ is the corresponding orientation block pair, one for test fingerprint and another for template fingerprint, respectively, $N$ is the number of overlapped blocks of both fingerprints, and $S(B_i, B_j)$ is determined by Eq. (9).

The final matching score $M_s$ is computed as follows:

$$M_s = \omega_m M_m + \omega_o M_o, \tag{12}$$

where $(\omega_m, \omega_o)$ is a weight vector that specifies the weight associated with the minutia matching score $M_m$ and the orientation field matching score $M_o$.

## 4. Experimental results

The experiments reported in this paper have been conducted on the public domain collection of fingerprint images, DB3 in FVC2002. It comprises 800 fingerprint images of size $300 \times 300$ pixels captured at a resolution of 500 dpi, from 100 fingers (eight impressions per finger).

A set of experiments have been conducted in order to show that both minutia information and orientation field information are complementary. First, denote our algorithm using only minutia information by A, which means to calculate matching score with Eq. (10); label our algorithm making use of both the minutia and orientation

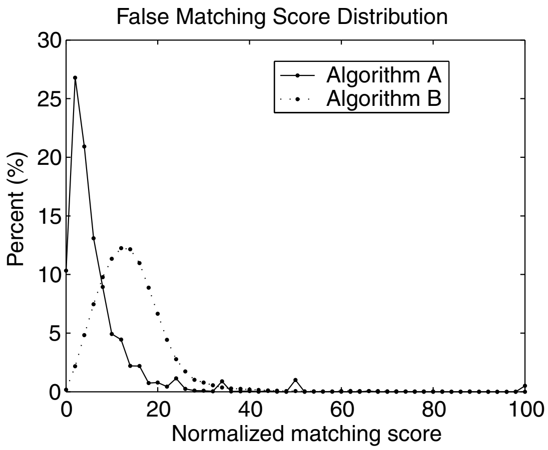


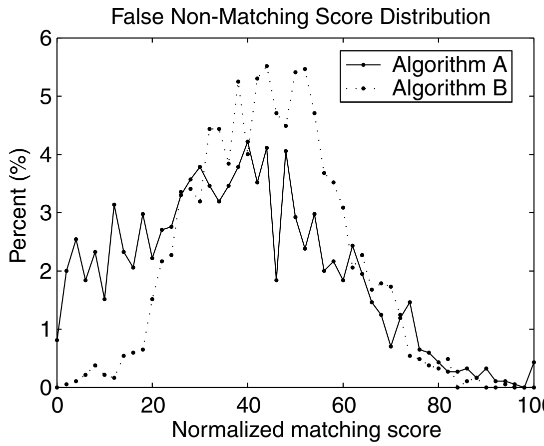


Fig. 2. The distribution curves of matching score on DB3 obtained with the algorithm A (solid line) and the algorithm B (dotted line).

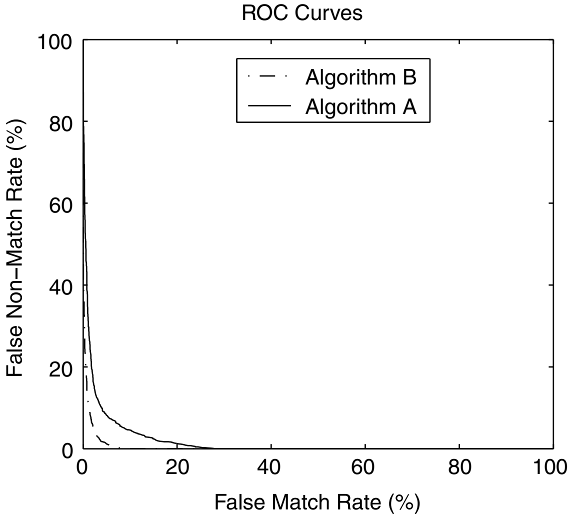


Fig. 3. ROC-curves on DB3 attained with the algorithm A (solid line) and the algorithm B (dash-dot line).

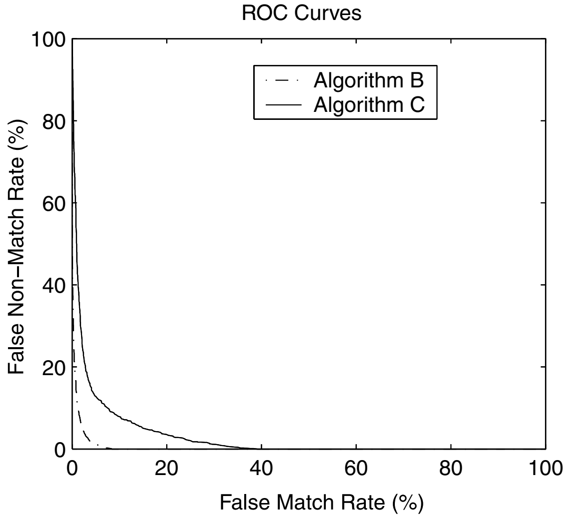


Fig. 4. ROC-curves on DB3 gotten with the algorithm C (solid line) and the algorithm B (dash-dot line).

field as B, which computes the matching score according to Eq. (12). Matching experiments have been performed on DB3 using algorithm A and algorithm B. The distributions of false matching and false non-matching scores are shown in Fig. 2. The Receiver Operating Characteristic (ROC) curves obtained by the two algorithms are illustrated in Fig. 3. We note that algorithm B outperforms the algorithm A. The only difference between the two algorithms consists of the method used for matching score computation. Consequently, these results reveal that the minutia information and orientation field information are complementary.

Secondly, for convenience we denote our algorithm utilizing only the orientation field information by C, which calculates the matching score according to Eq. (11). We compared the performance of the algorithm B with that of algorithm C on DB3. The comparative results are shown in Fig. 4 in terms of ROC curves. It is shown in the figure that algorithm B performs better than algorithm C. This is reasonable because the algorithm C only uses fingerprint orientation information.

Thirdly, we conducted a set of experiments on DB3 meant to compare our algorithm B with the approach proposed in (Jiang and Yau, 2000), which matches fingerprints based on both the local and global structures of minutiae. For convenience we label the method in (Jiang and Yau, 2000) as D. The algorithm D uses the local minutia structures for registration and computes matching score based on the similarity level of corresponding local structures. We have performed the two algorithms on DB3 and obtained the results expressed in

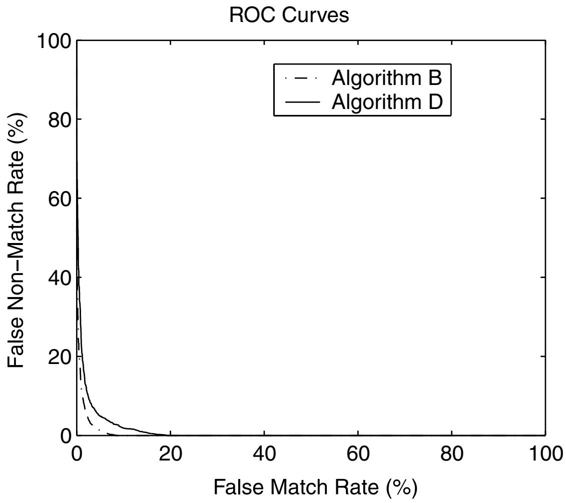


Fig. 5. ROC-curves on DB3 obtained with our matching method B (dash-dot line) and the algorithm D (solid line).

Table 1
Comparison of our algorithm with algorithm PA45

| Algorithm | EER (%) | FMR 100 (%) | FMR 1000 (%) | Zero FMR (%) | Average enroll time (s) | Average match time (s) |
|---|---|---|---|---|---|---|
| Our algorithm | 3.01 | 12.43 | 40.90 | 63.89 | 0.81 | 0.03 |
| PA45 | 3.48 | 5.46 | 8.00 | 9.21 | 0.37 | 0.44 |

terms of ROC curves, as shown in Fig. 5. The results demonstrate that our method B is more effective than algorithm D.

Finally, in Table 1 we compare our result with that of the algorithm called PA45 in FVC2002 on DB3 and obtaining the tenth place ranked by the equal error rate (EER). According to the ranking rule in terms of EER in FVC2002, our algorithm is in the first 10 places.

## 5. Conclusions

In this paper, we define novel minutia feature vectors that allow integration of orientation field information with the minutia details of fingerprints. The new feature vectors are rotation and translation invariant and capture more global information on fingerprint ridges and furrows pattern. Furthermore, it reduces the interdependencies between minutia details, which can be missed or erroneously detected by a minutia extraction algorithm. A new fingerprint matching algorithm that relies on the proposed minutia vectors has been developed. The orientation field and minutiae are combined to compute the matching score. The experiments show that the two kinds of information are complementary and the method for computing matching score is effective.

The usefulness of our proposed approach is confirmed in the experiments conducted, which show good performance.

## References

Almansa, A., Cohen, L., 2000. Fingerprint image matching by minimization of a thin-plate energy using a two-step algorithm with auxiliary variables. In: Fifth IEEE Workshop on Applications of Computer Vision. December 4–6, pp. 35–40.

Bazen, A.M., Gerea, S.H., 2002. Thin-plate spline modeling of elastic deformations in fingerprints. In: Proc. 3rd IEEE Benelux Signal Processing Symposium, pp. 1–4.

Chen, Z., Kuo, C.H., 1991. A topology-based matching algorithm for fingerprint authentication. In: Proc. 125th Annual IEEE Int. Carnahan Conference on Security Technology, pp. 84–87.

Hrechak, A.K., McHugh, J.A., 1990. Automatic fingerprint recognition using structural matching. Pattern Recognit. 23 (8), 893–904.

Jain, A.K., Hong, L., Pankanti, S., Bolle, R., 1997a. An identity-authentication system using fingerprint. Proc. IEEE 85 (9), 1365–1388.

Jain, A.K., Hong, L., Bolle, R., 1997b. On-line fingerprint verification. IEEE Trans. Pattern Anal. Machine Intell. 19 (4), 302–313.

Jiang, X., Yau, W.Y., 2000. Fingerprint minutiae matching based on the local and global structures. In: Proc. 15th Int. Conf. Pattern Recognit. 2, pp. 1038–1041.

Ratha, N.K., Karu, K., Chen, S., Jain, A.K., 1996. A real-time matching system for large fingerprint database. IEEE Trans. Pattern Anal. Machine Intell. 18 (8), 799–813.

Ross, A., Jain, A.K., Reisman, J., 2003. A hybrid fingerprint matcher. Pattern Recognit. 36, 1661–1673.

Wahab, A., Chin, S.H., Tan, E.C., 1998. Novel approach to automated fingerprint recognition. IEE Proc. Visual Image Signal Process. 145 (3), 160–166.